Electronic Supplementary Material (ESI) for Physical Chemistry Chemical Physics.

SUPPORTING INFORMATION

ClO-driven degradation of graphene oxide: new insights from DFT calculations

S. L. Romo-Ávila, D. Márquez-Ruíz, and R. A. Guirado-López*

[1]*Instituto de Física, Universidad Autónoma de San Luis Potosí, Álvaro Obregón 64, San Luis Potosí, SLP., 78000, México*

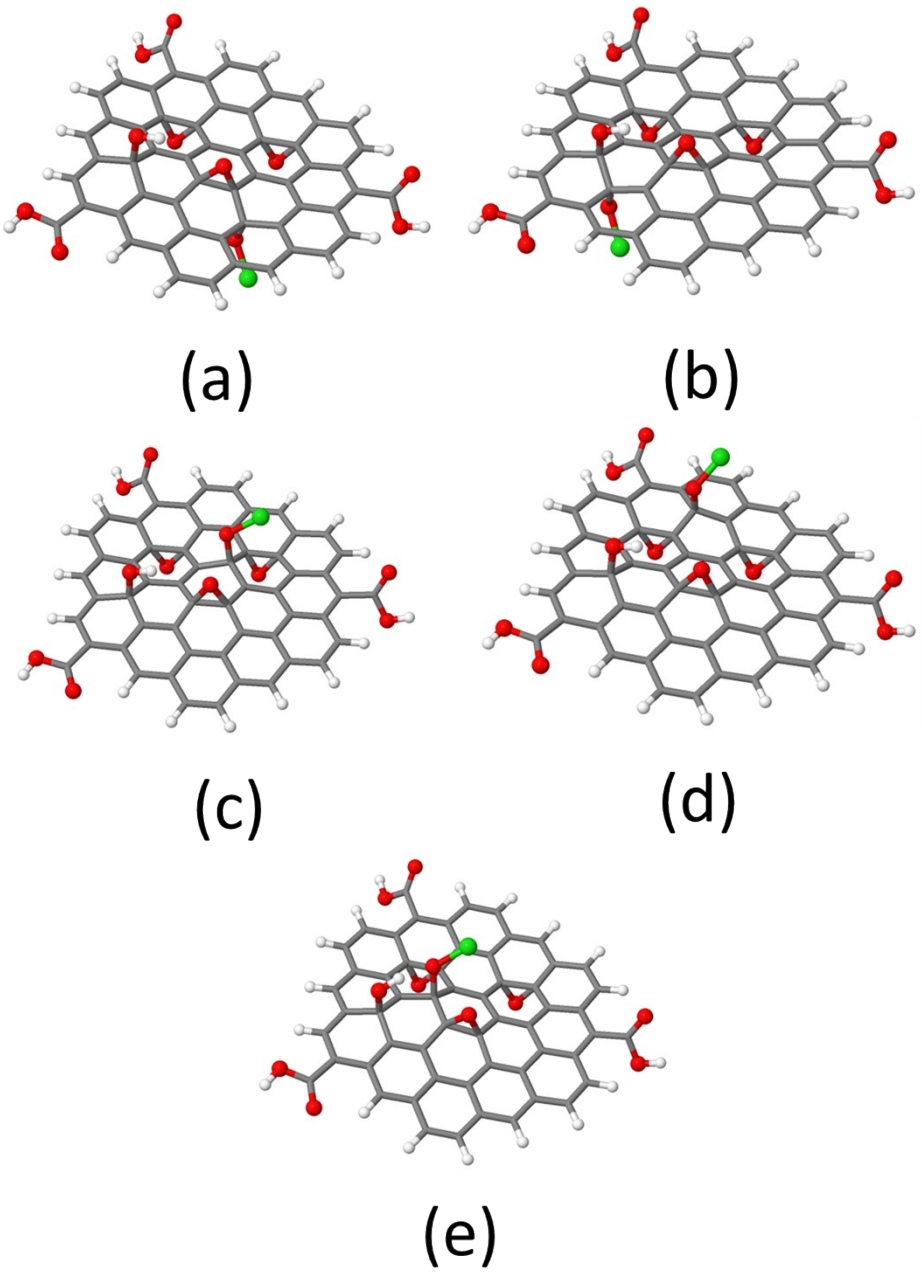

Figure S1. (a)—(e) Additional low-energy atomic configurations for the model $C_{54}H_{15}O_3OH(COOH)_3$ GO sheet shown in Fig. 1(e) interacting with a single ClO species adsorbed in different positions (see text).

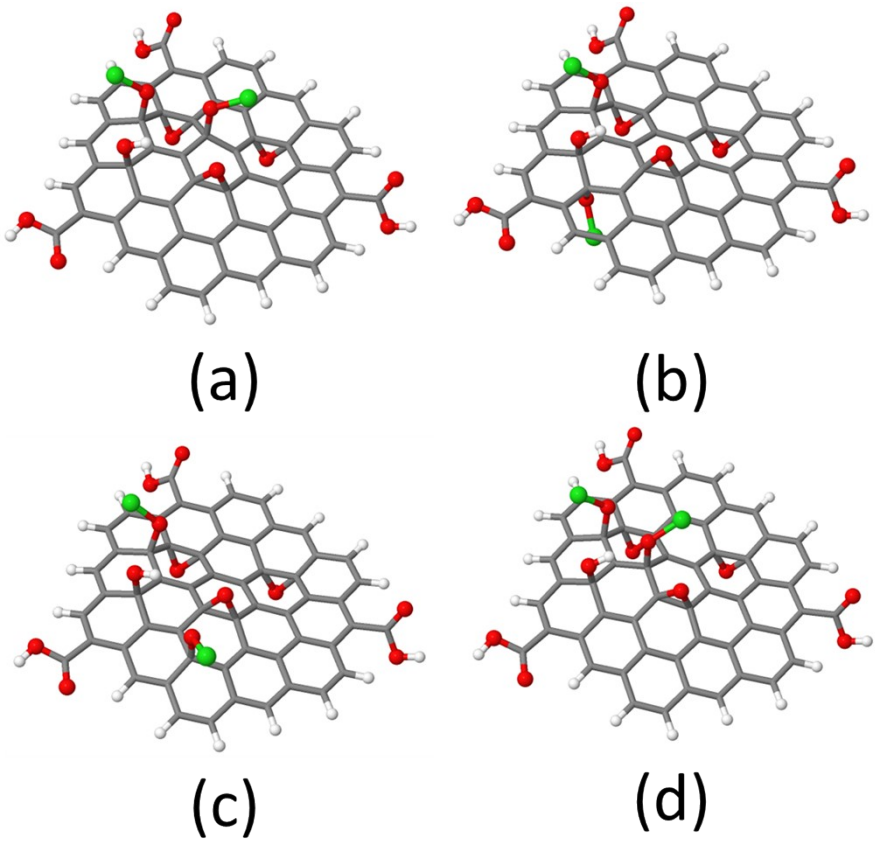

Figure S2. (a)—(d) Additional low-energy atomic configurations for the model $C_{54}H_{15}O_3OH(COOH)_3$ GO sheet shown in Fig. 1(e) interacting with two ClO species adsorbed in different positions (see text).

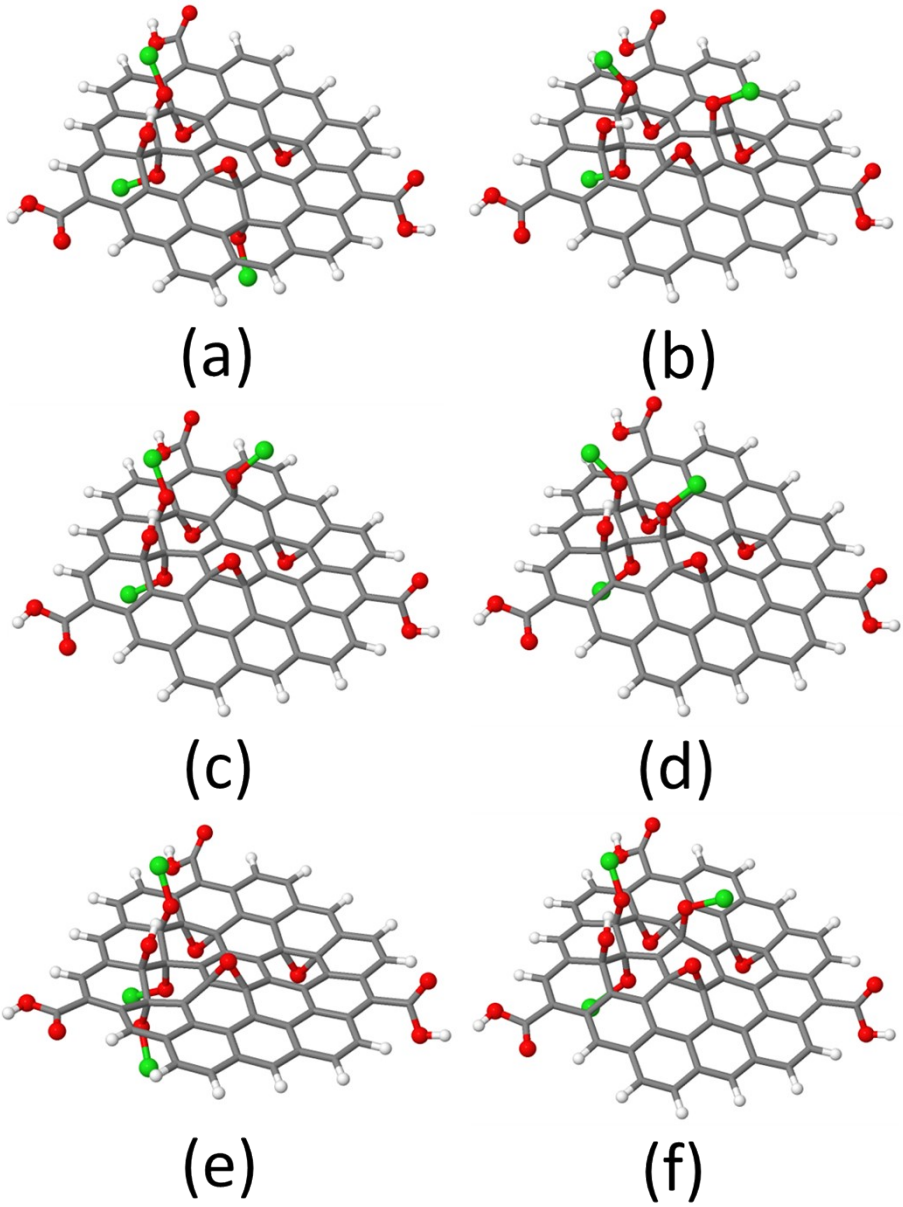

Figure S3. (a)—(f) Low-energy atomic configurations for the model $C_{54}H_{15}O_3OH(COOH)_3$ GO sheet shown in Fig. 1(e) interacting with three ClO species adsorbed in different positions (see text).

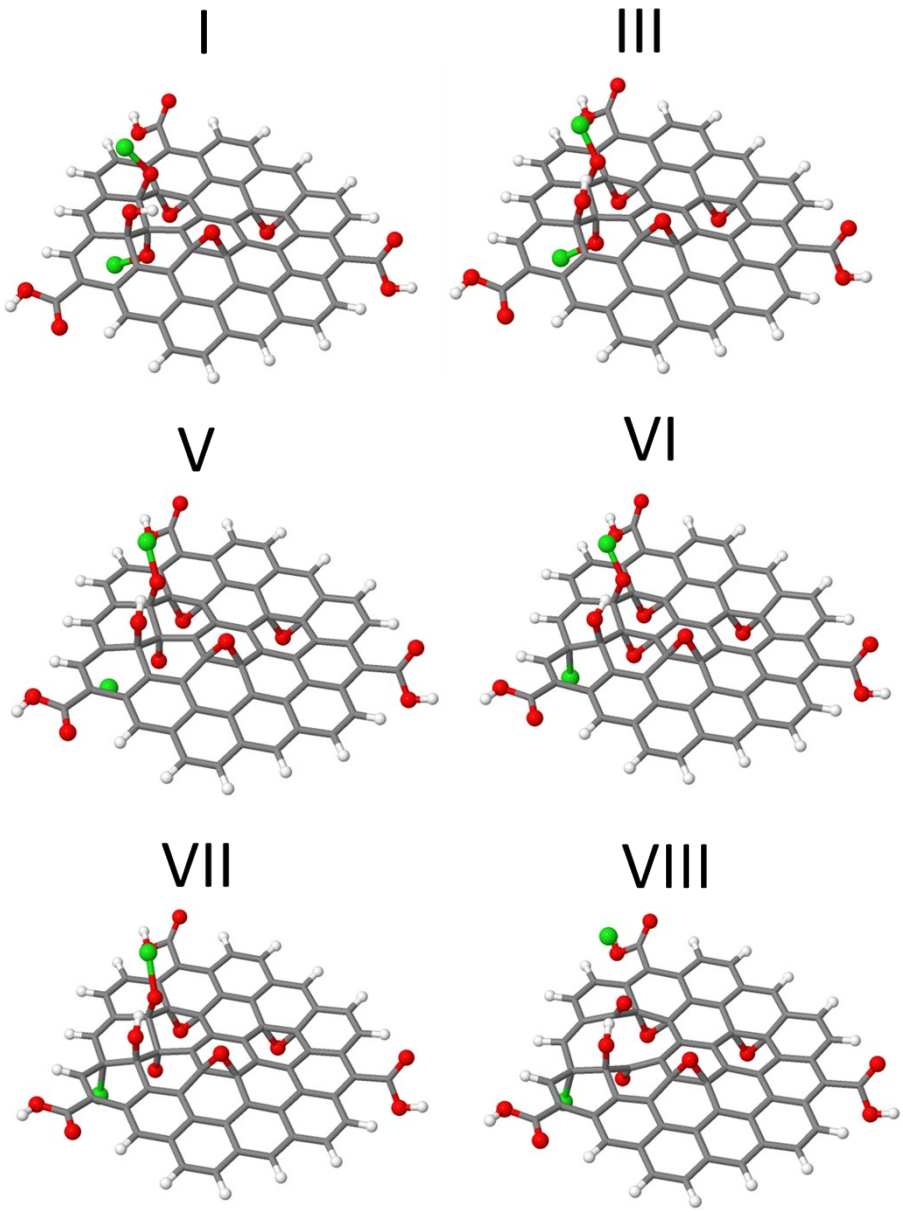

Figure S4. Selected images of the reaction path plotted in Fig. 4.

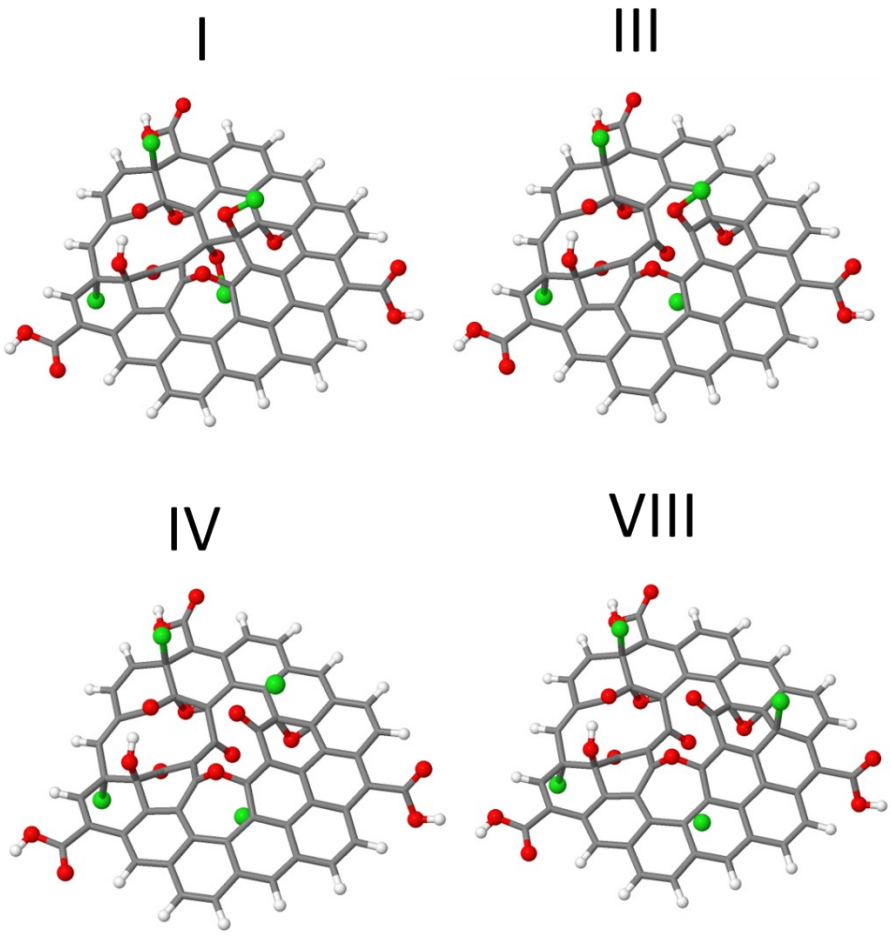

Figure S5. Selected images of the reaction path plotted in Fig. 5.

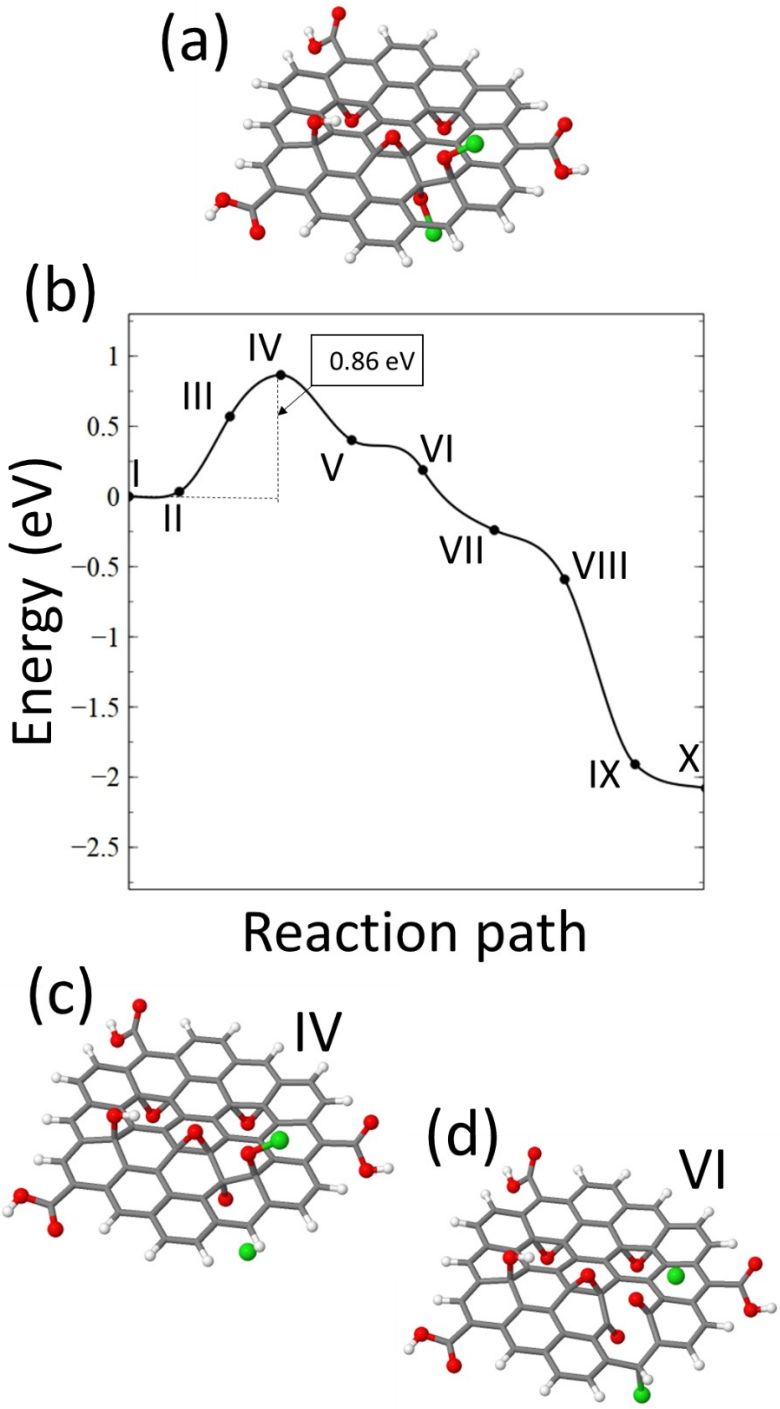

Figure S6. (a) A third scenario for the initial adsorbed configuration of the $Cl_{up}O_{up}/Cl_{down}O_{down}$ pair. (b) Reaction path (ten images) starting for the initial atomic array shown in (a). In (c) and (d) we present the atomic structure for images IV and VI (see text). We also include in the figure the calculated value of the energy barrier (eV).

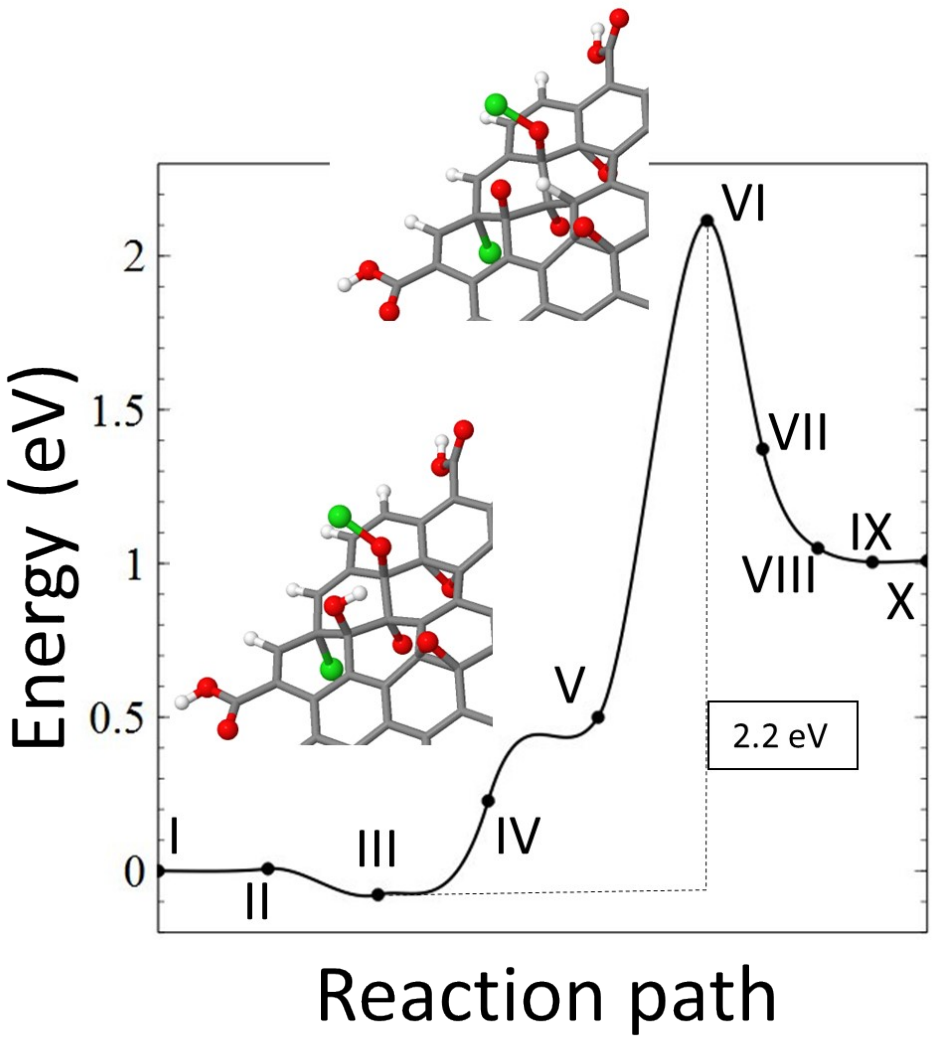

Figure S7. Reaction path (ten images) connecting the stable initial (image I) and final (image X) atomic configurations shown in Fig. S8. As insets, we present the atomic structure for images V (bottom inset) and VI (upper inset) (see text). We also include the calculated value of the energy barrier (in eV) required to achieve O_{up}—H_{up} bond dissociation.

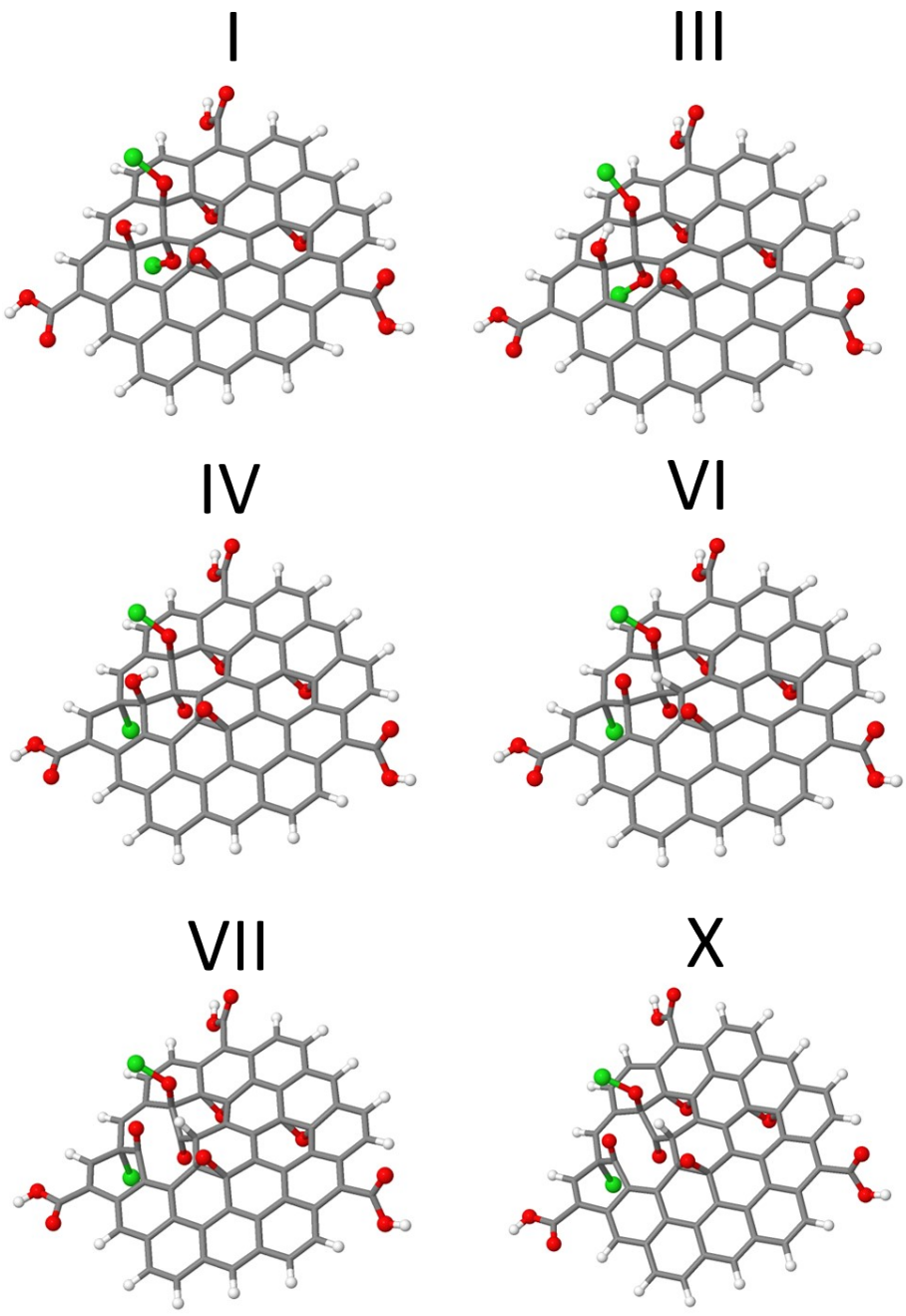

Figure S8. Selected images of the reaction path plotted in Fig. S7.

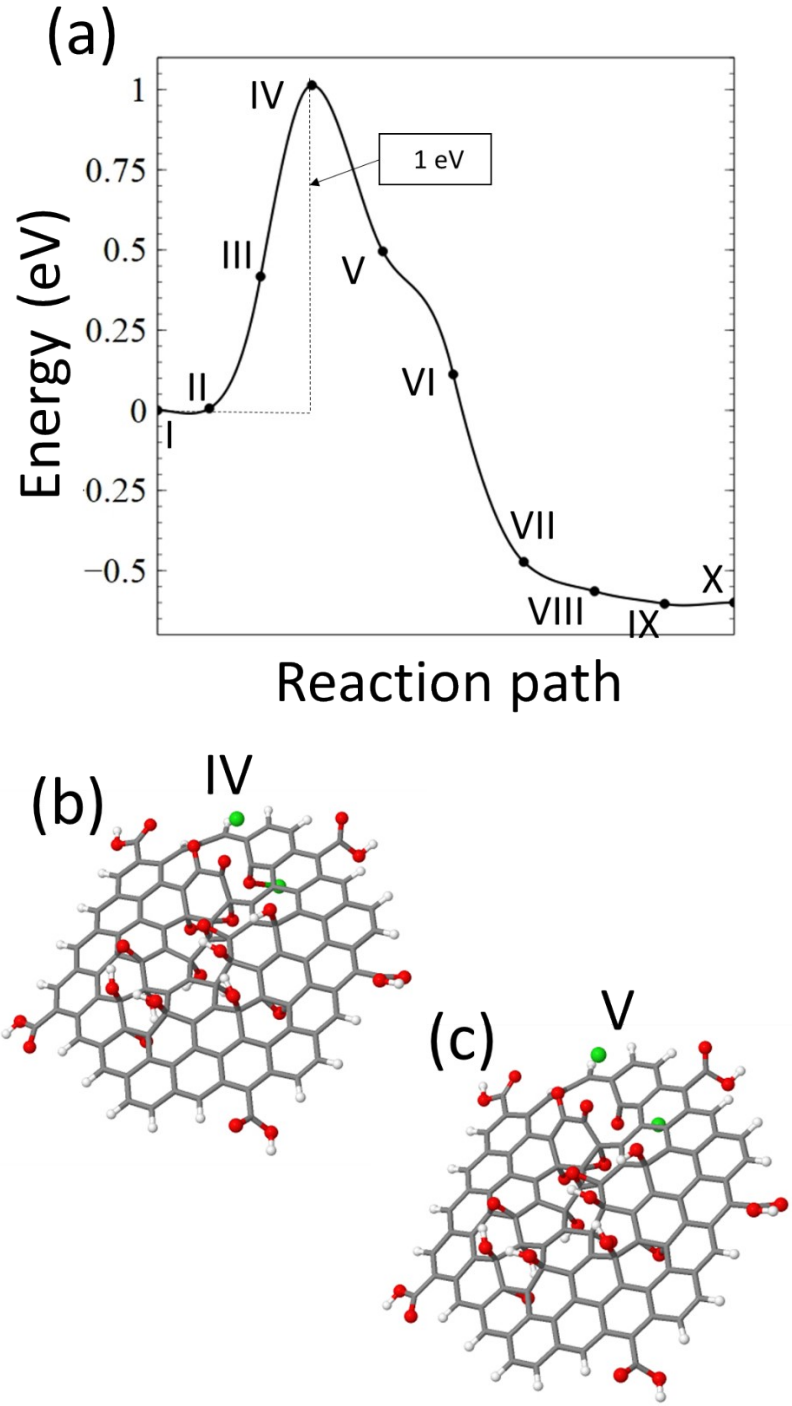

Figure S9. (a) Reaction path (ten images) connecting the stable initial (image I) and final (image X) atomic configurations shown in Figs. 7(a) and 7(b), respectively. In (b) and (c) we present the atomic structure for images IV and V (see text). We also include in the figure the calculated value of the energy barrier (in eV).

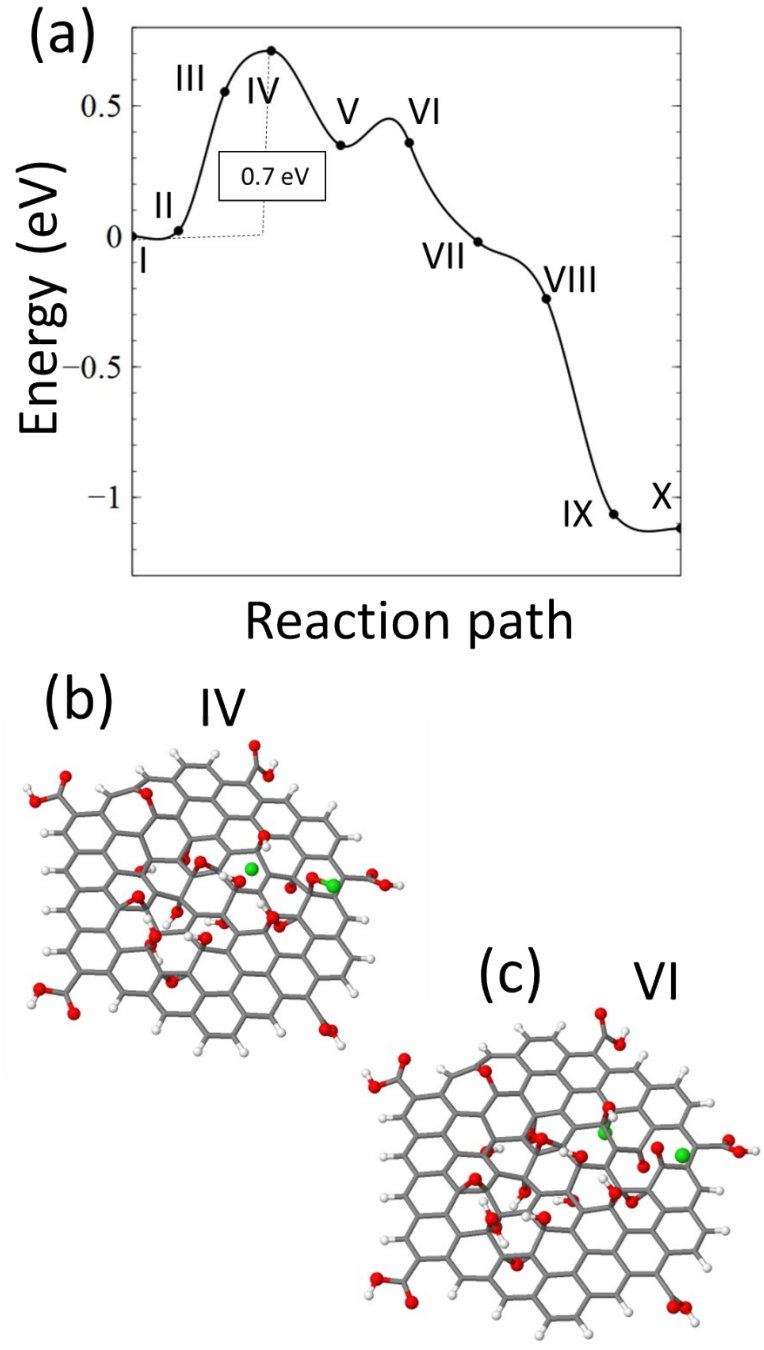

Figure S10. (a) Reaction path (ten images) connecting the stable initial (image I) and final (image X) atomic configurations shown in Figs. 7(c) and 7(d), respectively. In (b) and (c) we present the atomic structure for images IV and VI (see text). We also include in the figure the calculated value of the energy barrier (in eV).

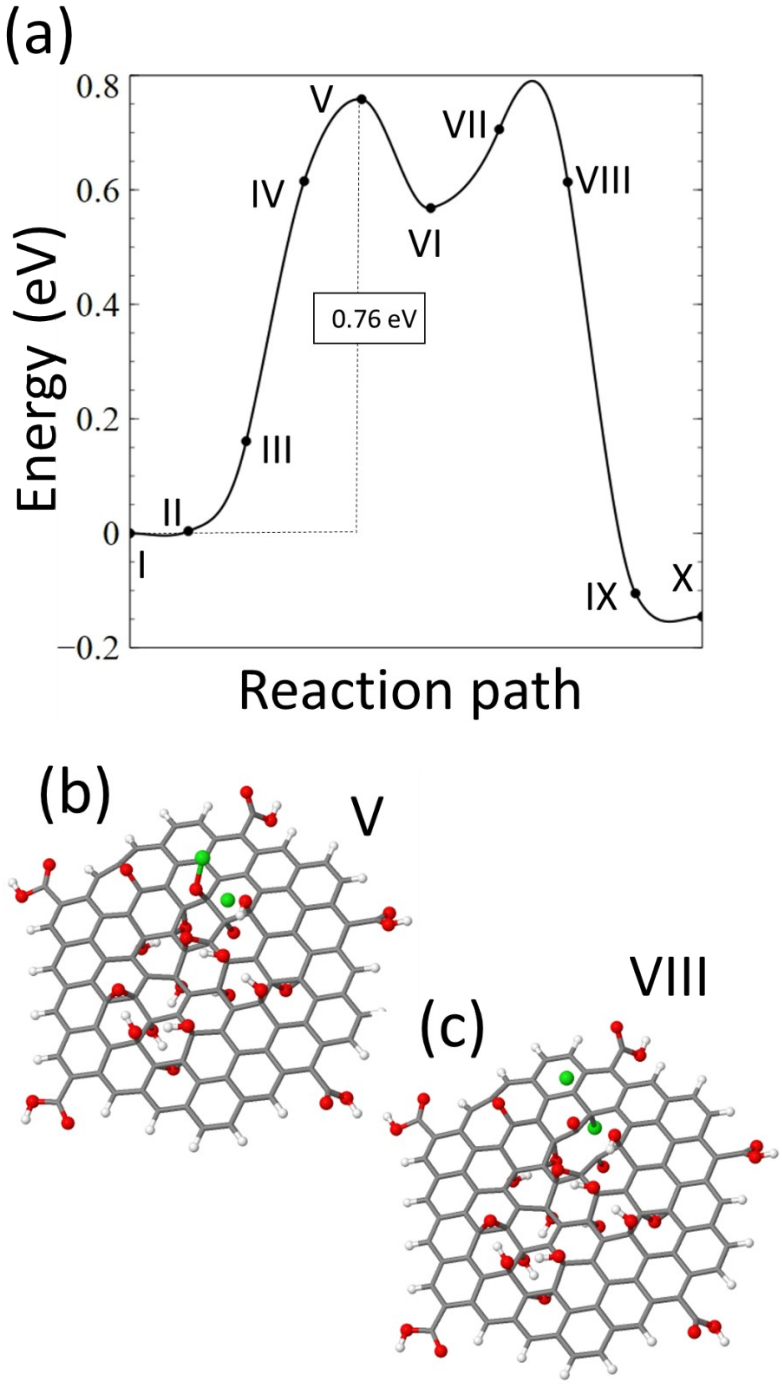

Figure S11. (a) Reaction path (ten images) connecting the stable initial (image I) and final (image X) atomic configurations shown in Figs. 7(e) and 7(f), respectively. In (b) and (c) we present the atomic structure for images V and VIII (see text). We also include in the figure the calculated value of the first energy barrier (eV).

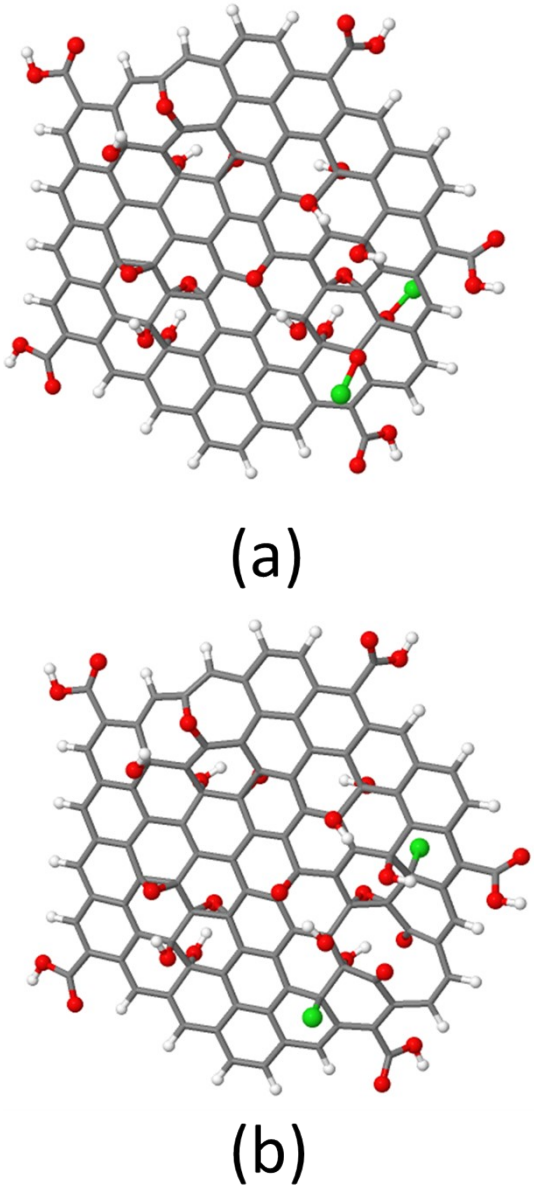

Figure S12. We show in (a) and (b) a second sequence of $Cl_{up}O_{up}/Cl_{down}O_{down}$ pair to carbonyl pair dissociation reactions and its impact on the structure of the model $C_{96}H_{19}O_6(OH)_9(COOH)_5$ GO layer shown in Fig. 2(c).

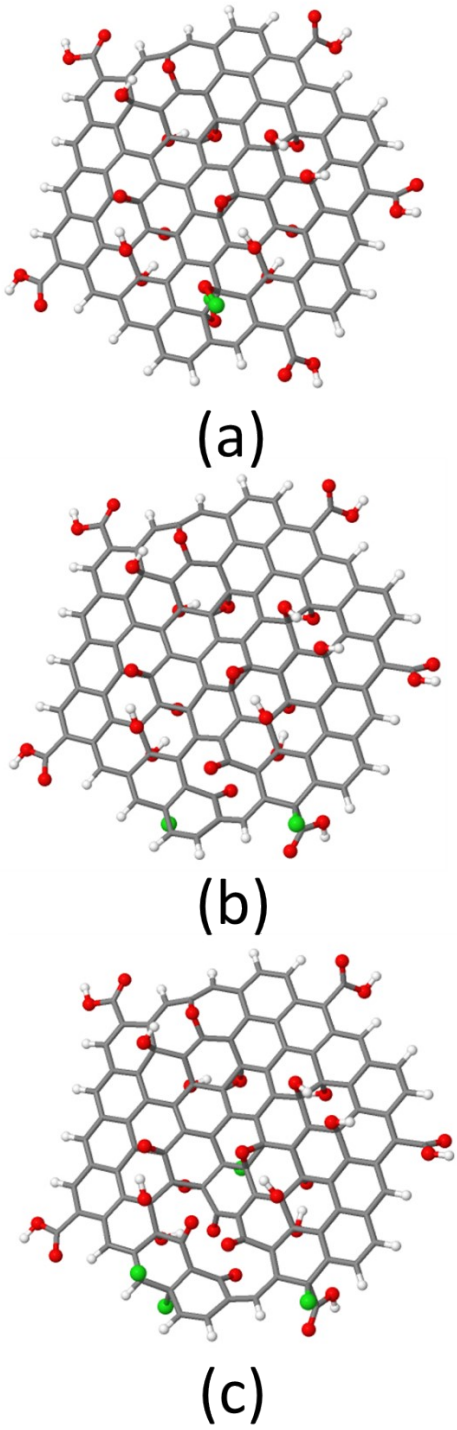

Figure S13. We show in (a)—(c) a third sequence of $Cl_{up}O_{up}/Cl_{down}O_{down}$ pair to carbonyl pair dissociation reactions and its impact on the structure of the model $C_{96}H_{19}O_6(OH)_9(COOH)_5$ GO layer shown in Fig. 2(c).

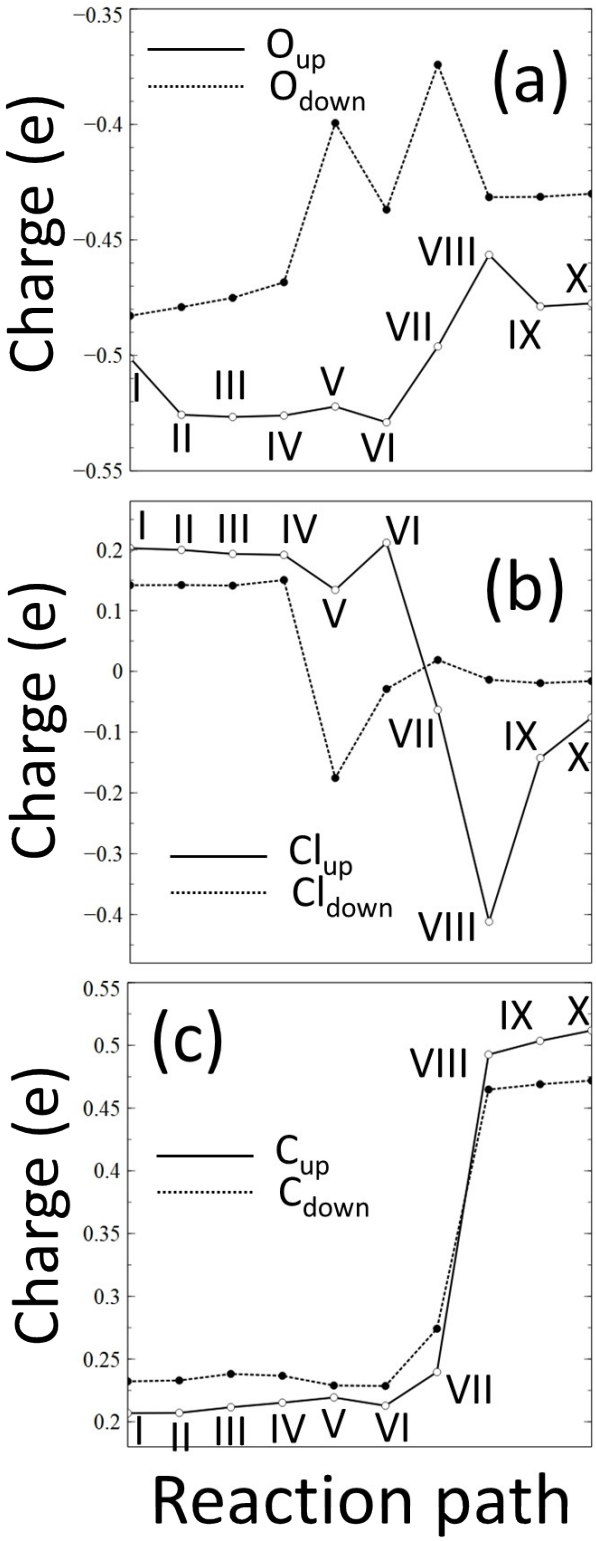

Figure S14. Distribution of local charges at selected (a) O, (b) Cl, and (c) C atoms all along the reaction path shown in Fig. 4 (see text).

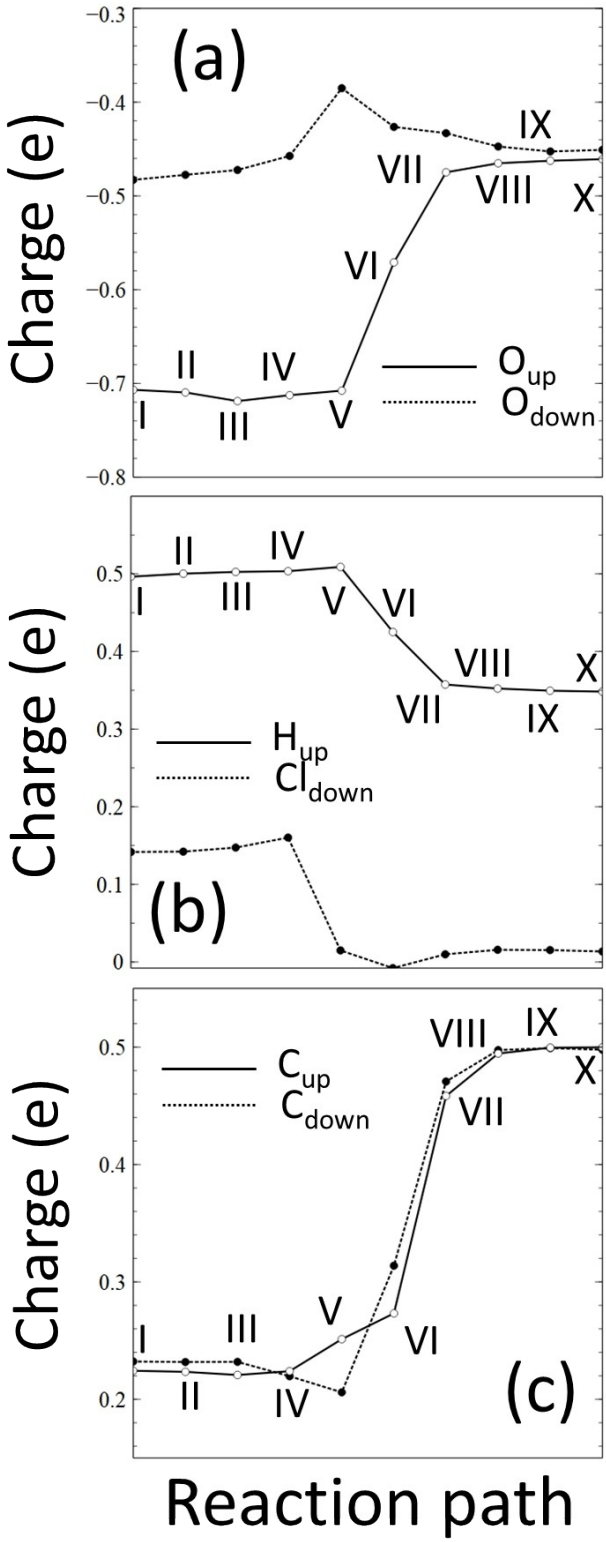

Figure S15. Distribution of local charges at selected (a) O, (b) Cl and H, as well as (c) C atoms all along the reaction path shown in Fig. S6 (see text).